

Nonequilibrium components in the region of very low transverse momentum in high-energy nuclear collisions

Yuuka Kanakubo ^{1,*}, Yasuki Tachibana ^{2,†} and Tetsufumi Hirano ^{1,‡}

¹*Department of Physics, Sophia University, Tokyo 102-8554, Japan*

²*Akita International University, Yuwa, Akita-city 010-1292, Japan*



(Received 1 August 2022; accepted 30 September 2022; published 18 November 2022)

We analyze Pb + Pb collisions at $\sqrt{s_{NN}} = 2.76$ TeV with a novel framework based on the dynamical core-corona picture that describes particle productions from both equilibrium and nonequilibrium components. We remark on the possibility of the contribution from nonequilibrium components in the very low transverse momentum (p_T) region and show that such contributions significantly affect p_T -integrated four-particle cumulants. These results strongly suggest the necessity of nonequilibrium components when one extracts properties of the quark-gluon plasma from experimental data using sophisticated dynamical models based on relativistic hydrodynamics.

DOI: [10.1103/PhysRevC.106.054908](https://doi.org/10.1103/PhysRevC.106.054908)

I. INTRODUCTION

Properties of the quark-gluon plasma (QGP) [1–3], the primordial matter of our universe, have been investigated through relativistic heavy-ion collision experiments at the Relativistic Heavy Ion Collider (RHIC) and Large Hadron Collider (LHC). Since the discovery of the nearly perfect fluidity of the QGP solidified the applicability of relativistic hydrodynamics [4–7], one of the main streams of the theoretical QGP study has been led by multistage dynamical models in which relativistic hydrodynamics plays a central role in describing the dynamics of the QGP. Since then, there have been several splendid theoretical developments of the dynamical models.

The particle spectra in the low transverse momentum region ($p_T \lesssim 5$ GeV) are commonly understood as thermal distributions boosted by the radial velocity of expansion, which can be described by theoretical descriptions based on relativistic hydrodynamics: dynamical models with the hydrodynamic description of the QGP (for a review, see, e.g., Ref. [8]) or the blast wave model [9]. However, contrary to the common understanding, it has also been widely discussed that there is a significant lack of particle production in hydrodynamic models in the very low p_T region ($p_T \lesssim 1$ GeV/ c) compared to experimental data. Back in the late 1990s, the possible interpretations of the discrepancy at very low p_T were suggested: the existence of pion condensation [10], effects of nonchemical equilibrium [11,12], and contribution from resonance decays with the blast wave model [13] and the hydrodynamic simulation [14]. Although it seemed that the issue was almost resolved by the above works at that time, it has been still reported that the state-of-the-art hydrodynamic models cannot describe the particle yields at the very low p_T at LHC energies even if Bayesian parameter estimation or global fit are performed [15,16]. Thus, to our best knowledge, no successful interpretation has been made of the spectra in the very low p_T region, while several interpretations are suggested as possible solutions [17–22]. Therefore, other promising mechanisms are required to explain the excess of particle yields in experimental data over conventional hydrodynamic models.

In this paper, we investigate this problem with the dynamical core-corona initialization framework (DCCI2) [23]. This framework was built aiming for a comprehensive description of high-energy nuclear collisions from small to large colliding systems, i.e., proton-proton (p - p) to heavy-ion (A - A) collisions. In this framework, dynamical aspects of the core-corona picture [24] are attained by the novel dynamical initialization framework [25,26]. Under the core-corona picture [24], the systems generated in high-energy nuclear collisions are described with two components: the core (equilibrated matter) and the corona (nonequilibrated matter). The hadronic production from the core components exhibits the boosted equilibrium distribution, while the corona components undergo string fragmentation in a vacuum. In our previous work [23], we found a nontrivial interplay between the core and the corona components in p_T spectra of charged hadrons in minimum bias Pb + Pb collisions. As expected, the core components are dominant in $p_T \lesssim 4$ GeV/ c due to the QGP fluid formation, while the corona components, which are the leading hadrons originating from the hard partons, are dominant in high p_T regions. Surprisingly, it turns out that the corona components reach $\approx 20\%$ below $p_T \approx 1$ GeV. These soft hadrons are fragmented from strings consisting of hard partons. Such a non-negligible contribution to the particle productions from corona components at midrapidity gives a certain correction to observables obtained purely from core components described by hydrodynamics.

As expected, the core components are dominant in $p_T \lesssim 4$ GeV/ c due to the QGP fluid formation, while the corona components, which are the leading hadrons originating from the hard partons, are dominant in high p_T regions. Surprisingly, it turns out that the corona components reach $\approx 20\%$ below $p_T \approx 1$ GeV. These soft hadrons are fragmented from strings consisting of hard partons. Such a non-negligible contribution to the particle productions from corona components at midrapidity gives a certain correction to observables obtained purely from core components described by hydrodynamics.

*y-kanakubo-75t@eagle.sophia.ac.jp

†ytachibana@aiu.ac.jp

‡hirano@sophia.ac.jp

In this paper, using DCCI2, we analyze the “soft from corona” components in particle-identified hadron p_T spectra and the centrality dependence of p_T spectra of charged pions and elucidate the effects of the corona components on the four-particle cumulant, $c_2\{4\}$, in Pb + Pb collisions at $\sqrt{s_{NN}} = 2.76$ TeV. Throughout this paper, we use the natural units, $\hbar = c = k_B = 1$.

II. MODEL

The dynamical separation into the core and corona components is realized by implementing the core-corona picture into the dynamical initialization framework [23,27,28]. Under this framework, initial conditions of relativistic hydrodynamics are dynamically generated via source terms of hydrodynamic equations. With the assumption that the system is described with the QGP fluids (the core) and the nonequilibrated partons (the corona) and that the energy and momentum are conserved as a summation of the two components, energy and momentum deposited from nonequilibrated partons become the sources of QGP fluids.

The entire flow of DCCI2 [23] is summarized as follows: The system produced at the initial state is described by phase-space distributions of initially produced partons obtained from PYTHIA8.244 [29] with switching off hadronization on an event-by-event basis. The heavy-ion mode of PYTHIA, PYTHIA8 ANGANTYR [30,31], is used for simulations of heavy-ion collisions. At a formation time, $\tau_0 = 0.1$ fm, of initially generated partons, dynamical initialization of the QGP fluids based on the core-corona picture starts and the system is getting separated into the core and corona components. For the space-time evolution of the core, ideal hydrodynamic simulations are performed in the $(3 + 1)$ -dimensional Milne coordinates [32] incorporating $s95p-v1.1$ [33], the equation of state constructed with a seamless connection of the $(2 + 1)$ -flavor lattice QCD at high temperature and a hadron resonance gas model at low temperature. The particlization of fluids is performed with IS3D [34], a Monte Carlo sampler converting hydrodynamic fields on the hypersurface at the switching temperature, $T_{sw} = 0.165$ GeV, into hadrons. The nonequilibrated partons undergo hadronization through the Lund string fragmentation with PYTHIA8. The hadrons obtained from both switching hypersurface and string fragmentation are handed to the hadronic transport model, JAM [35], to perform hadronic rescatterings and resonance decays.

In the following, we denote as “full DCCI2 simulations” all steps mentioned above. To see a breakdown of the total yields into the core and the corona components, we switch off hadronic rescatterings in JAM and perform only resonance decays. This is because hadronic rescatterings mix up the two components in the late stage of reactions. We also have an option of “the core components with hadronic rescatterings” in which we neglect the corona components from string fragmentation in the hadronic cascade and mimic the results from conventional hybrid models in which hydrodynamic evolution is followed by the hadronic afterburner.

Note that we minorly updated the following three parameters of DCCI2 simulations from Ref. [23] to improve

description of p_T spectra in central Pb + Pb collisions at $\sqrt{s_{NN}} = 2.76$ TeV: the parameter regulating cross sections of multiparton interactions and infrared QCD emissions in initial parton generation, p_{T0Ref} , the coefficient of the cross section of the collision between two partons in the dynamical core-corona initialization σ_0 , and the transverse width of the Gaussian distribution used in the smearing of deposited energy and momentum in the dynamical generation of the QGP fluids, σ_\perp . In this paper, we use $p_{T0Ref}(p + p) = 1.9$ GeV, $p_{T0Ref}(\text{Pb} + \text{Pb}) = 1.0$ GeV, $\sigma_0 = 0.3$ fm², and $\sigma_\perp = 0.6$ fm, which do not alter the conclusion significantly in Ref. [23].¹ Details of the other parameters can be found in Ref. [23].

III. RESULTS

First, we investigate the fraction of core and corona contributions in p_T spectra of charged pions, charged kaons, and protons and antiprotons in central and mid-central collisions in Pb + Pb collisions at $\sqrt{s_{NN}} = 2.76$ TeV to capture the overall tendency. Second, the comparisons of p_T spectra between experimental data and results from DCCI2 are shown to quantify the contribution of the corona components in the very low p_T region. Finally, we also elucidate the effect of the corona components in the very low p_T region on the four-particle cumulant, $c_2\{4\}$, as a function of multiplicity, N_{ch} .

Figure 1 shows p_T spectra of charged pions, charged kaons, and protons and antiprotons in $|\eta| < 0.8$ at 0–5% and 40–60% centrality classes in Pb + Pb collisions at $\sqrt{s_{NN}} = 2.76$ TeV. The hadronic rescatterings are switched off in JAM to investigate the contribution from core and corona components. As an overall tendency for all particle-identified hadrons and centrality, the core and corona contributions are dominant in lower and higher p_T , respectively. This is exactly the consequence of the implementation of the dynamical core-corona picture: partons with lower momentum tend to deposit energy and momentum and the ones with higher momentum tend to survive in the QGP fluids.

The classification of centrality and particle identification, which were not made in our previous paper [23], reveal further dynamics. Regarding the core components, the slopes of p_T spectra of core components become slightly flatter in more central events for all hadron species, which originates from the generation of stronger radial flows in more central events. The fraction of the core components compared to the corona components is larger in more central events, which is also a consequence of the implementation of the core-corona picture. As a result, the dominance of the core components reaches up to higher p_T in more central events for all hadron species. This tendency is strongly seen in heavier particles such as protons and antiprotons since heavier particles in the core components acquire larger p_T due to the mass effect of radial expansion [37]. This leads to the core dominance of

¹Although we will not discuss results in $p + p$ collisions in this paper, we denote them $p_{T0Ref}(p + p)$ for the sake of comparison.

protons spanning up to $p_T \approx 6$ GeV in 0–5% centrality class.²

Now we focus on the contribution from the corona components in the very low p_T region. The corona contribution is getting more significant for lower p_T in $p_T \lesssim 1$ GeV, which is the same tendency as in Fig. 5(b) in Ref. [23]. This behavior can be naively understood as a consequence of the interplay between two different shapes of the spectra: approximately an exponential function $\approx e^{-p_T/T}$ ($T > 0$) and a power-law function $\approx 1/p_T^n$ ($n > 0$) for the core and the corona components, respectively. Contrary to the exponential spectra that linearly decrease with p_T in the semilogarithmic plot, the slope of the power law spectra increases with decreasing p_T and can be steeper than the exponential spectra towards $p_T \rightarrow 0$ GeV. This leads to a rather nontrivial p_T dependence of the fraction of the core and the corona components and the relative increase of the corona contributions compared to the core contributions at such very low p_T . Since the fraction of the corona components increases with decreasing p_T -integrated yields at midrapidity [23] for the more peripheral collisions, the larger contributions from the corona components are at very low p_T for all hadron species. Even when we focus on 0–5% central events, the relative increase of the corona contributions at very low p_T still remains and the fraction of the corona components is even larger in heavier particle spectra. Notably, the fraction of the corona components of protons and antiprotons reaches $\approx 50\%$ at $p_T \rightarrow 0$ GeV in 0–5% central events. These tendencies are all understood as a consequence of interplay between the blueshift of the core spectra for heavy particles and the “soft from corona” components from fragmentation of strings consisting of hard partons.

Figure 2 shows p_T spectra of charged pions, charged kaons, and protons and antiprotons in $|\eta| < 0.8$ from DCCI2 compared with ALICE experimental data [36] in Pb + Pb collisions at $\sqrt{s_{NN}} = 2.76$ TeV. In addition to the results from full DCCI2 simulations, the results from the core components with hadronic rescatterings are shown for comparison in the upper panels of Fig. 2. This makes it possible to quantify how much the corona contribution to full DCCI2 simulations compensates for the discrepancy between the experimental data and the results from conventional hybrid models. Shown in the upper panels are the insets to enlarge the very low p_T regions in which the corona components are expected to contribute. In the corresponding lower panels, the ratios of the ALICE experimental data to results with full DCCI2 simulation and to the core components with hadronic rescatterings are shown for each p_T bin.

We first observe that the ALICE experimental data cannot be reproduced solely by the core components with hadronic

rescatterings in the very low p_T region in all cases, which is consistent with previous findings in hydrodynamic models [15,16]. The results from full DCCI2 simulations show better agreement with experimental data than those of the core components with hadronic rescatterings. Results from full DCCI2 simulations still lack pion yields in the very low p_T regions. On the other hand, the corona contributions fill the discrepancy in the very low p_T region between the experimental data and the results from the core components with hadronic rescatterings in the case of kaons and protons. Therefore one can say that the contribution from the corona components would be one of the strong clues to resolving a long-standing issue of discrepancy between experimental data and hydrodynamic models.

From Figs. 1 and 2, conventional hydrodynamic models without the corona contribution reasonably work to describe p_T -differential observables in the intermediate p_T region ($1 \lesssim p_T \lesssim 3$ GeV). However, p_T -integrated observables such as mean p_T and anisotropic flow coefficients v_n can be largely affected by the contribution from the corona components. To see this, we further investigate the effects of corona contributions on flow observables. Figures 3(a) and 3(b) show four-particle cumulants, $c_2\{4\}$, as functions of charged particle multiplicity, N_{ch} , in Pb + Pb collisions at $\sqrt{s_{NN}} = 2.76$ TeV. Here $c_2\{4\}$ is decomposed into four-particle correlation, $\langle\langle 4 \rangle\rangle$, and two-particle correlation, $\langle\langle 2 \rangle\rangle$:

$$c_n\{4\} = \langle\langle 4 \rangle\rangle - 2(\langle\langle 2 \rangle\rangle)^2, \quad (1)$$

$$\langle\langle m \rangle\rangle = \frac{\sum_e M_e P_m \langle m \rangle_e}{\sum_e M_e P_m}, \quad (2)$$

$$\langle 4 \rangle_e = \frac{\sum_{i \neq j \neq k \neq l} e^{in(\phi_i + \phi_j - \phi_k - \phi_l)}}{M_e P_4}, \quad (3)$$

$$\langle 2 \rangle_e = \frac{\sum_{i \neq j} e^{in(\phi_i - \phi_j)}}{M_e P_2}, \quad (4)$$

where ϕ_i is an azimuthal angle of the i th particle in the e th event and M_e is the number of charged particles in a kinematic range in that event [38]. The m -permutation of M_e , $M_e P_m$, is defined as $M_e P_m = M_e! / (M_e - m)!$. Charged particle multiplicity, N_{ch} , is obtained by counting the number of charged particles with $|\eta| < 0.8$ and $0.2 < p_T < 3.0$ GeV, which is the same kinematic range used in Ref. [39]. There is no eta gap imposed in this analysis since we checked that there is no significant difference in results between with and without eta gap in Pb + Pb collisions. In general, four-particle cumulants, $c_2\{4\}$, are negative when the second order anisotropic flow is finite [38]. In fact, we have checked that PYTHIA8 ANGANTYR, which does not contain any secondary scattering effects in the default settings, predicts almost zero-consistent $c_2\{4\}$ as expected.

In Fig. 3(a), $c_2\{4\}$ from simulations without hadronic rescatterings and ones from core and corona contributions are shown for comparison. The results without hadronic rescatterings and the core contributions show negative $c_2\{4\}$ above $N_{ch} \approx 10^2$, which manifests a clear signal of anisotropic collective behavior. On the other hand, the corona contributions show zero-consistent $c_2\{4\}$ within statistical error bars for

²The dynamical initialization generates random initial transverse flow due to momentum conservation of initially generated partons [25]. This results in a broad range of radial flow velocity at the switching hypersurface compared to conventional hydrodynamic simulation with vanishing initial transverse flow. Consequently, the core components are blueshifted by various radial flow velocities, and the resulting p_T slope in the higher p_T region tends to reflect the large radial push at the dynamical initialization.

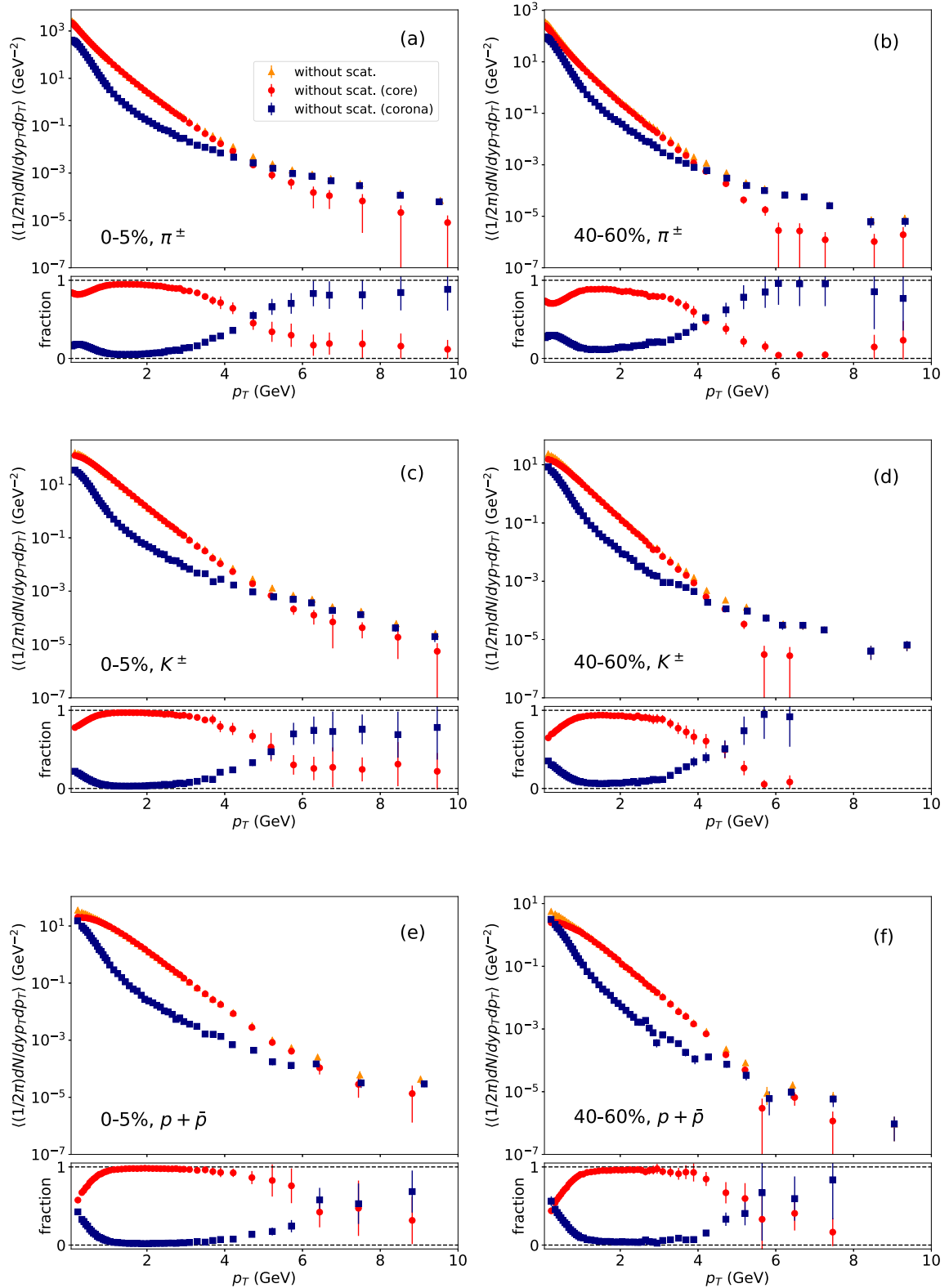


FIG. 1. Transverse momentum spectra of charged pions in (a) 0–5% and (b) 40–60%, charged kaons in (c) 0–5% and (d) 40–60%, and protons and antiprotons in (e) 0–5% and (f) 40–60% centrality classes, in Pb + Pb collisions at $\sqrt{s_{NN}} = 2.76$ TeV from DCC12. Upper: Results with switching off hadronic rescatterings (orange squares) and their breakdown into core (red triangles) and corona contributions (blue circles) are shown. Lower: Fraction of the core R_{core} (red circles) and that of the corona R_{corona} (blue squares) components in each p_T bin.

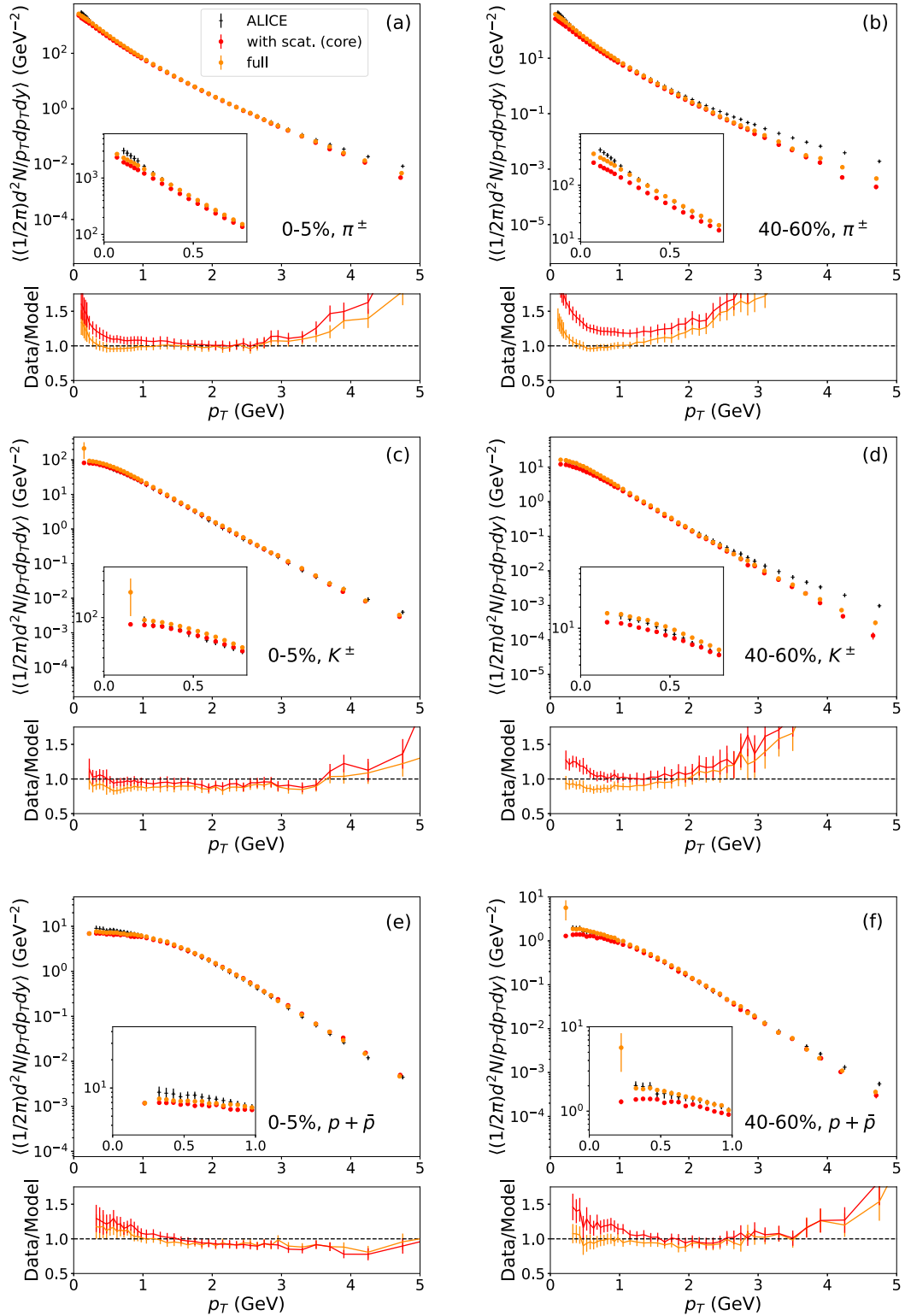


FIG. 2. Transverse momentum spectra of charged pions in (a) 0–5% and (b) 40–60%, charged kaons in (c) 0–5% and (d) 40–60%, and protons and antiprotons in (e) 0–5% and (f) 40–60% centrality classes, in Pb + Pb collisions at $\sqrt{s_{NN}} = 2.76$ TeV from DCCI2. Upper: Results from full DCCI2 simulations (orange circles) and the core components with hadronic rescatterings (red circles) are compared with ALICE experimental data (black crosses). Insets are enlarged plots focusing on very low p_T regions. Lower: Ratios of the ALICE experimental data [36] to results from full DCCI2 simulation (orange) and core components with hadronic rescatterings (red) at each p_T bin.

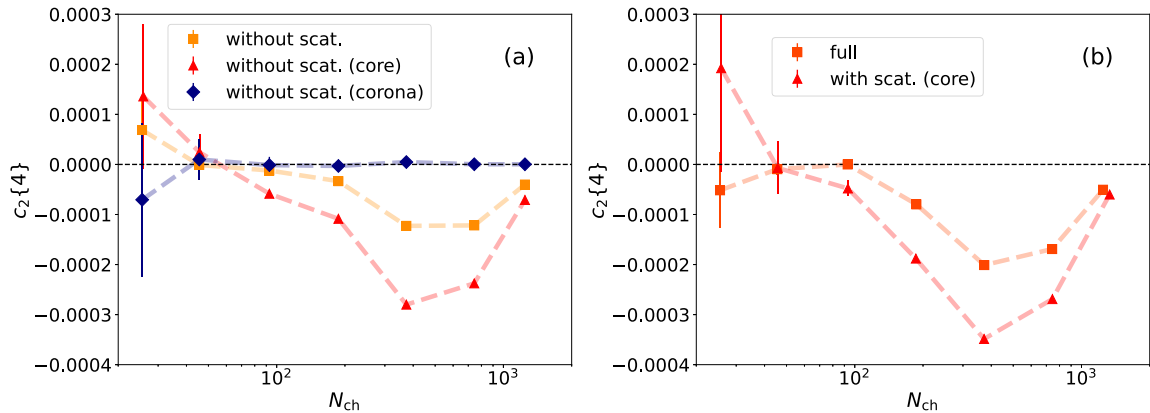


FIG. 3. Four-particle cumulants for charged hadrons as functions of the number of produced charged hadrons in Pb + Pb collisions at $\sqrt{s_{NN}} = 2.76$ TeV. (a) Results only from the core (red diamonds) and the corona (blue diamonds) components as a breakdown of results without hadronic rescatterings (orange squares) are shown. (b) Results from full DCC12 simulations (squares) and the core components with hadronic rescatterings (triangles) are shown. Dashed lines are drawn as a guide to the eyes.

the entire range of N_{ch} . This clearly demonstrates that multiparticle cumulants are essential indicators for hydrodynamic behaviors of the produced matter. We point out that the absolute values of $c_2\{4\}$ solely from the core contributions are diluted to the one without hadronic rescatterings due to the existence of the corona contributions. As shown in Eq. (2), the multiparticle correlation $\langle\langle m \rangle\rangle$ is the correlation per permutation of m particles. Even if there is a subensemble of particles with no correlations among them which does not contribute to the numerator in Eq. (2), those particles are counted in the permutation of m particles in the denominator in Eq. (2).³ Thus, one can interpret this result as an indication that the correlation originating from the core contributions is diluted by the corona contributions mainly due to more permutations of particles. This brings us to the conclusion that flow coefficients obtained from conventional hydrodynamic or hybrid models should not be compared with experimental data as long as the nonequilibrium contribution that is distinct from the hydrodynamic (core) components exists in the system.

Figure 3(b) shows the comparisons of $c_2\{4\}$ from full DCC12 simulations and that from core contributions with hadronic rescatterings. Compared to the results in Fig. 3(a), one sees that the hadronic rescatterings slightly enhance the absolute values of $c_2\{4\}$ for both results due possibly to the generation of extra anisotropic flow in the late hadronic stage. It turns out that there still exists a clear difference between these two results even after rescatterings of hadrons are taken into account in the late hadronic stage. Therefore the existence of the corona components clearly affects four-particle cumulants as a p_T -integrated observable.

IV. SUMMARY

We analyzed Pb + Pb collisions at $\sqrt{s_{NN}} = 2.76$ TeV from DCC12 and quantified the corona contributions to particle-identified p_T spectra in central and peripheral events. We found the relative increase of the corona contributions below $p_T \approx 1$ GeV in both central and peripheral events. The blue shift of the core spectra, due to the mass of particles, results in a relative increase of corona contributions in very low p_T regions. Especially, we found that the proton and antiproton p_T spectra in the central events show $\approx 50\%$ of the corona contributions in the very low p_T region ($p_T \approx 0$ GeV). From the comparisons between experimental data and results from DCC12, we concluded that the corona contributions can be a possible candidate to compensate for the lack of yields obtained from conventional hydrodynamic or hybrid models below $p_T \approx 0.5$ GeV. We also showed that the corona contributions in the very low p_T region dilute four-particle cumulants $c_2\{4\}$ obtained purely from the core contributions. This result suggests the necessity of the implementation of the corona components to more precisely extract transport coefficients of the QGP from comparisons between dynamical models and experimental data by using Bayesian parameter estimation [15,40–48].

We admit that there is still a slight lack of very low p_T yields, as shown in Fig. 2. On the one hand, there might be other particle production mechanisms at such low p_T as discussed in previous studies, for example, the existence of pion condensation [19] or the effect of critical chiral fluctuations [22]. On the other hand, this can also be highly related to the underestimation of high p_T yields in our model compared to the experimental data, which can be attributed to the lack of N_{coll} scaling in PYTHIA8 ANGANTYR or the absence of a sophisticated jet quenching mechanism. Since the relative increase of the very low p_T yields is due to fragmentation of strings including hard corona partons, it is necessary to

³Of course, we are aware that there might exist correlations between the main ensemble (the core) and the subensemble (the corona). We simply assume those correlations do not contribute to the numerator.

improve the description of initial parton production in the high p_T regions in nucleus-nucleus collisions for more quantitative discussions.

ACKNOWLEDGMENT

The work by Y.K. is supported by JSPS KAKENHI Grant No. 20J20401.

-
- [1] J. C. Collins and M. J. Perry, *Phys. Rev. Lett.* **34**, 1353 (1975).
 [2] N. Cabibbo and G. Parisi, *Phys. Lett. B* **59**, 67 (1975).
 [3] E. V. Shuryak, *Sov. Phys. JETP* **47**, 212 (1978).
 [4] U. W. Heinz and P. F. Kolb, in *Statistical QCD, proceedings, international symposium, bielefeld*, Germany, August 26–30, 2001 [*Nucl. Phys. A* **702**, 269 (2002)].
 [5] M. Gyulassy and L. McLerran, in *Quark gluon plasma, new discoveries at RHIC: A case of strongly interacting quark gluon plasma, proceedings, RBRC workshop*, Brookhaven, Upton, NY, May 14–15, 2004 [*Nucl. Phys. A* **750**, 30 (2005)].
 [6] E. V. Shuryak, in *Quark gluon plasma, new discoveries at RHIC: A case of strongly interacting quark gluon plasma, proceedings, RBRC Workshop*, Brookhaven, Upton, NY, May 14–15, 2004 [*Nucl. Phys. A* **750**, 64 (2005)].
 [7] T. Hirano and M. Gyulassy, *Nucl. Phys. A* **769**, 71 (2006).
 [8] C. Shen, *EPJ Web Conf.* **259**, 02001 (2022).
 [9] E. Schnedermann, J. Sollfrank, and U. W. Heinz, *Phys. Rev. C* **48**, 2462 (1993).
 [10] J. Zimanyi, G. I. Fai, and B. Jakobsson, *Phys. Rev. Lett.* **43**, 1705 (1979).
 [11] M. Kataja and P. V. Ruuskanen, *Phys. Lett. B* **243**, 181 (1990).
 [12] S. Gavin and P. V. Ruuskanen, *Phys. Lett. B* **262**, 326 (1991).
 [13] J. Sollfrank, P. Koch, and U. W. Heinz, *Z. Phys. C* **52**, 593 (1991).
 [14] U. Ornik and R. M. Weiner, *Phys. Lett. B* **263**, 503 (1991).
 [15] G. Nijs, W. van der Schee, U. Gürsoy, and R. Snellings, *Phys. Rev. Lett.* **126**, 202301 (2021).
 [16] D. Devetak, A. Dubla, S. Floerchinger, E. Grossi, S. Masciocchi, A. Mazeliauskas, and I. Selyuzhenkov, *J. High Energy Phys.* **06** (2020) 044.
 [17] V. Begun, W. Florkowski, and M. Rybczynski, *Phys. Rev. C* **90**, 014906 (2014).
 [18] V. Begun, W. Florkowski, and M. Rybczynski, *Phys. Rev. C* **90**, 054912 (2014).
 [19] V. Begun and W. Florkowski, *Phys. Rev. C* **91**, 054909 (2015).
 [20] P. Huovinen, P. M. Lo, M. Marzenko, K. Morita, K. Redlich, and C. Sasaki, *Phys. Lett. B* **769**, 509 (2017).
 [21] A. Guillen and J.-Y. Ollitrault, *Phys. Rev. C* **103**, 064911 (2021).
 [22] E. Grossi, A. Soloviev, D. Teaney, and F. Yan, *Phys. Rev. D* **104**, 034025 (2021).
 [23] Y. Kanakubo, Y. Tachibana, and T. Hirano, *Phys. Rev. C* **105**, 024905 (2022).
 [24] K. Werner, F.-M. Liu, and T. Pierog, *Phys. Rev. C* **74**, 044902 (2006).
 [25] M. Okai, K. Kawaguchi, Y. Tachibana, and T. Hirano, *Phys. Rev. C* **95**, 054914 (2017).
 [26] C. Shen and B. Schenke, *Phys. Rev. C* **97**, 024907 (2018).
 [27] Y. Kanakubo, M. Okai, Y. Tachibana, and T. Hirano, *Prog. Theor. Exp. Phys.* **2018**, 121D01 (2018).
 [28] Y. Kanakubo, Y. Tachibana, and T. Hirano, *Phys. Rev. C* **101**, 024912 (2020).
 [29] T. Sjöstrand, S. Mrenna, and P. Z. Skands, *Comput. Phys. Commun.* **178**, 852 (2008).
 [30] C. Bierlich, G. Gustafson, and L. Lönnblad, *J. High Energy Phys.* **10** (2016) 139.
 [31] C. Bierlich, G. Gustafson, L. Lönnblad, and H. Shah, *J. High Energy Phys.* **10** (2018) 134.
 [32] Y. Tachibana and T. Hirano, *Phys. Rev. C* **90**, 021902(R) (2014).
 [33] P. Huovinen and P. Petreczky, *Nucl. Phys. A* **837**, 26 (2010).
 [34] M. McNelis, D. Everett, and U. Heinz, *Comput. Phys. Commun.* **258**, 107604 (2021).
 [35] Y. Nara, N. Otuka, A. Ohnishi, K. Niita, and S. Chiba, *Phys. Rev. C* **61**, 024901 (1999).
 [36] J. Adam *et al.* (ALICE Collaboration), *Phys. Rev. C* **93**, 034913 (2016).
 [37] T. Hirano and Y. Nara, *Phys. Rev. C* **69**, 034908 (2004).
 [38] N. Borghini, P. M. Dinh, and J.-Y. Ollitrault, *Phys. Rev. C* **63**, 054906 (2001).
 [39] S. Acharya *et al.* (ALICE Collaboration), *Phys. Rev. Lett.* **123**, 142301 (2019).
 [40] J. E. Bernhard, P. W. Marcy, C. E. Coleman-Smith, S. Huzurbazar, R. L. Wolpert, and S. A. Bass, *Phys. Rev. C* **91**, 054910 (2015).
 [41] J. E. Bernhard, J. S. Moreland, S. A. Bass, J. Liu, and U. Heinz, *Phys. Rev. C* **94**, 024907 (2016).
 [42] J. Auvinen, J. E. Bernhard, S. A. Bass, and I. Karpenko, *Phys. Rev. C* **97**, 044905 (2018).
 [43] J. E. Bernhard, J. S. Moreland, and S. A. Bass, *Nat. Phys.* **15**, 1113 (2019).
 [44] D. Everett *et al.* (JETSCAPE Collaboration), *Phys. Rev. C* **103**, 054904 (2021).
 [45] D. Everett *et al.* (JETSCAPE Collaboration), *Phys. Rev. Lett.* **126**, 242301 (2021).
 [46] G. Nijs, W. van der Schee, U. Gürsoy, and R. Snellings, *Phys. Rev. C* **103**, 054909 (2021).
 [47] J. Auvinen, K. J. Eskola, P. Huovinen, H. Niemi, R. Paatelainen, and P. Petreczky, *Phys. Rev. C* **102**, 044911 (2020).
 [48] J. E. Parkkila, A. Onnerstad, and D. J. Kim, *Phys. Rev. C* **104**, 054904 (2021).